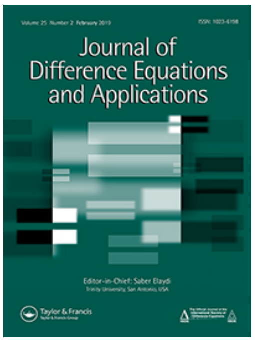

Journal of Difference Equations and Applications

ISSN: 1023-6198 (Print) 1563-5120 (Online) Journal homepage: https://www.tandfonline.com/loi/gdea20

High accuracy two-level implicit compact difference scheme for 1D unsteady biharmonic problem of first kind: application to the generalized Kuramoto–Sivashinsky equation

R. K. Mohanty & Deepti Kaur

JOURNAL OF DIFFERENCE EQUATIONS AND APPLICATIONS
2019, VOL. 25, NO. 2, 243–261
https://doi.org/10.1080/10236198.2019.1568423

Taylor & Francis
Taylor & Francis Group

High accuracy two-level implicit compact difference scheme for 1D unsteady biharmonic problem of first kind: application to the generalized Kuramoto–Sivashinsky equation

R. K. Mohanty [a] and Deepti Kaur [b]

[a]Department of Applied Mathematics, Faculty of Mathematics and Computer Science, South Asian University, Akbar Bhawan, Chanakyapuri, New Delhi, India; [b]Department of Mathematics, Maitreyi College, University of Delhi, New Delhi, India

ABSTRACT

We propose a two-level implicit high order compact scheme for the one-dimensional unsteady biharmonic problem of first kind. The values of ϕ and ϕ_x are prescribed on the boundary. Using a combination of values of ϕ and ϕ_x at each grid point, the difference formula is derived for the unsteady biharmonic equation without discretizing the boundary conditions. The proposed method has second order time accuracy and fourth order space accuracy using just three grid points of a single compact stencil at every time level. The first order space derivative is also computed with same accuracy as a by-product of the method. Using the Von-Neumann analysis, the derived scheme is shown to be unconditionally stable. With a slight modification, the proposed method is applicable to solve singular problems. The performance of the proposed scheme is illustrated by numerical experiments done on a collection of test problems having physical significance including the nonlinear Kuramoto–Sivashinsky equation.

ARTICLE HISTORY
Received 11 June 2018
Accepted 28 December 2018

KEYWORDS
Compact difference scheme; generalized Kuramoto–Sivashinsky equation; extended Fisher–Kolmogorov equation; block tri-diagonal matrices; unconditional stability; singularity

AMS SUBJECT CLASSIFICATIONS
65M06; 65M12; 65M22

1. Introduction

In this work, we propose and implement a high order compact difference scheme to solve the following fourth order time-dependent partial differential equation (PDE):

$$\frac{\partial^4\phi}{\partial x^4} = f(x, t, \phi, \phi_t, \phi_x, \phi_{xx}, \phi_{xxx}), \quad (x, t) \in \Omega \tag{1}$$

subject to the initial condition

$$\phi(x, 0) = \phi_0(x), \quad a \le x \le b, \tag{2}$$

along with Dirichlet and Neumann boundary conditions of the type:

$$\phi(a, t) = g_0(t), \quad \phi(b, t) = g_1(t), \quad t > 0, \tag{3a}$$

CONTACT R. K. Mohanty rmohanty@sau.ac.in Department of Applied Mathematics, Faculty of Mathematics and Computer Science, South Asian University, Akbar Bhawan, Chanakyapuri, New Delhi110021, India

$$\frac{\partial \phi}{\partial x}(a,t) = h_0(t), \quad \frac{\partial \phi}{\partial x}(b,t) = h_1(t), \quad t > 0, \tag{3b}$$

where $\Omega \equiv \{(x,t)|\, a < x < b,\ t > 0\}$ and f, ϕ_0, g_0, g_1, h_0, h_1 are functions of sufficient smoothness. It is assumed that the solution $\phi(x,t)$ is smooth enough for maintaining the order and accuracy of the difference scheme under discussion. The PDE (1) along with the initial condition (2) and boundary conditions (3a)–(3b) are referred to as the 1D unsteady biharmonic problem of first kind. Equation (1) occurs in a wide class of problems in mathematical physics and engineering such as pattern formation, movement of a fluid going down a vertical wall, a spatially uniform oscillating chemical reaction in a homogeneous medium and unstable drift waves in plasmas, etc. (see [3,10,13,25]).

Of particular interest in this work is the generalized Kuraomoto–Sivashinsky (GKS) equation which is a model of nonlinear PDE often arising in the study of continuous media that exhibits a chaotic behaviour form:

$$\frac{\partial \phi}{\partial t} + \phi\frac{\partial \phi}{\partial x} + \alpha\frac{\partial^2 \phi}{\partial x^2} + \beta\frac{\partial^3 \phi}{\partial x^3} + \gamma\frac{\partial^4 \phi}{\partial x^4} = 0, \quad (x,t) \in \Omega, \tag{4}$$

where α, β and γ are real constants. Initially, Kuramoto and Tsuzuki [13] derived it in the mid-1970s for studying the dissipative structure of reaction-diffusion and then it was derived independently by Sivashinsky as a model for analysing flame front propagation during mild combustion processes and instabilities induced by thermal conduction of the considered gas [24]. The GKS equation also known as the KdV-Burgers-Kuramoto equation is significant in explaining various physical processes in unstable systems [25] and in the study of stress waves arising in porous media [23].

For $\beta = 0$, Equation (4) is referred as the Kuramoto–Sivashinsky (KS) equation:

$$\frac{\partial \phi}{\partial t} + \phi\frac{\partial \phi}{\partial x} + \alpha\frac{\partial^2 \phi}{\partial x^2} + \gamma\frac{\partial^4 \phi}{\partial x^4} = 0, \quad (x,t) \in \Omega \tag{5}$$

which is a fundamental fourth order PDE modelling various nonlinear physical phenomenon in unstable systems containing both second order and fourth order spatial derivatives in its linear part. Here, the constants α and γ are associated with the growth of linear stability and surface tension, respectively. The KS equation arises in a wide range of physical processes such as in representing long waves on the interface involving two viscous fluids [10], in flame propagation [24], in reaction-diffusion combustion dynamics and in the study of unstable drift waves in plasmas [13]. The KS equation comprises of high order dissipation term $\partial^4\phi/\partial x^4$, nonlinear advection $\phi(\partial\phi/\partial x)$ and linear growth term $\partial^2\phi/\partial x^2$. When $\gamma = 0$, the surface tension term is eliminated and the KS equation reduces to Burger's equation.

Due to the vast application of the GKS equation, considerable attention has been given to determine its analytical and numerical solutions. But the analytical treatment of this nonlinear differential equation is too involved a process so it is essential to develop efficient numerical methods whose solutions are important for scientists and engineers. In recent years, various techniques have been developed for the numerical solution of the GKS equation including finite difference methods [1,2], the tanh-function method [7], the local discontinuous Galerkin method [27], the Chebyshev spectral collocation method [12], the radial basis function based on the mesh free method [26], the quintic B-spline collocation scheme [16], the lattice Boltzmann model [14], the numerical technique derived from finite difference and collocation methods [15], the cubic Hermite collocation method [8] and the high order compact difference method [21]. Recently, Rashidinia and Jokar [22] proposed a numerical technique for the solution of the GKS equation based on the Crank–Nicolson method for temporal discretization together with the collocation method using the polynomial scaling functions in the spatial direction. The KS equation has been solved numerically by implementing a differential quadrature method with the quintic B-spline functions by Mittal and Dahiya [17].

The fourth order semilinear PDE of the form:

$$\frac{\partial \phi}{\partial t} + \gamma \frac{\partial^4 \phi}{\partial x^4} - \frac{\partial^2 \phi}{\partial x^2} + \phi^3 - \phi = 0, \quad (x,t) \in \Omega, \tag{6}$$

where γ is a positive constant and is a particular model of the type (1)–(3). For $\gamma = 0$, Equation (6) reduces to the Fisher–Kolmogorov equation in the standard form [3]. However, by adding a stabilizing fourth order derivative term to the Fisher–Kolmogorov equation, Dee and Van Saarlos [5] proposed the model expressed by Equation (6) and termed it as the extended Fisher–Kolmogorov (EFK) equation. The EFK equation arises in numerous applications ranging from travelling waves in reaction diffusion systems [3] to phase transition near a Lifshitz point [28]. Doss and Nandini [6] proposed a H^1-Galerkin mixed finite element cubic spline approximation method for the EFK equation (6) by means of a splitting technique. Danumjaya [4] studied finite element Galerkin methods for Equation (6) and discussed existence uniqueness results using the Lyapunov functional.

Among various finite difference methods, compact high order schemes which need less information from neighbouring grid points are gradually gaining popularity due to easy implementation and robustness of accuracy in the solution values. The advantage of developing a compact scheme is its suitability to be used directly adjacent to the boundary without introducing any ghost points to the computational domain. Compact high order schemes achieve high order accuracy without a significant increase in the grid size. In contrast, high order difference schemes formulated with non-compact stencil result in higher bandwidth of the coefficient matrix yielding more arithmetic operations which are not computationally attractive. Mohanty *et al.* [18] presented a fourth order accurate compact difference method for solving the two-dimensional nonlinear biharmonic equation with Dirichlet and Neumann boundary conditions. Recently, Mohanty and Kaur [19,20] derived three-level and two-level compact implicit finite difference formulas on a non-uniform grid for two different classes of nonlinear fourth order parabolic PDEs in one-space variable for which ϕ and ϕ_{xx} are known at the boundary.

Equations of type (1) of second kind, i.e. when ϕ and $\partial^2\phi/\partial n^2$ are prescribed at the boundary are decomposable to coupled second order equations; however, such type of reduction is not possible with first kind boundary conditions (3a)–(3b) so it is required to develop a high order compact approximation to the normal derivative. In this paper, we present the two-level implicit difference formula having second order time accuracy and fourth order space accuracy for the solution of nonlinear unsteady biharmonic equation (1). The developed scheme employs just three grid points at every time level resulting in compact formulation. Our technique includes discretizing the biharmonic equation using not only the solution value ϕ but also the value of the first order space derivative ϕ_x at all interior grid points without requiring any fictitious points for incorporating the boundary conditions. The given Dirichlet and Neumann boundary conditions are exactly satisfied without using any approximation for the derivative at the boundary. The resulting formula yields a block tri-diagonal matrix system to determine the solutions ϕ and ϕ_x at all grid points.

The remaining paper is organized as follows. In Section 2, we formulate and derive two-level implicit difference formula for the fourth order time-dependent PDE (1). Furthermore, using the von Neumann analysis, the proposed method is shown to be unconditionally stable for a linear equation in Section 3. In Section 4, we discuss the use of the suggested method for the one-space dimension unsteady biharmonic equation with singular coefficients, wherein the method is modified in such a way that the order and accuracy of the solution are maintained everywhere in the vicinity of the singularity. In Section 5, computational results are provided to demonstrate the practical implementation of the derived method. Computational results reveal that the present method offers better accuracy in comparison with the other existing work in the literature. Finally, concluding remarks are presented in Section 6.

2. Compact finite difference scheme

We consider an auxiliary variable $\psi(x,t) = \phi_x(x,t)$, so the PDE (1) can be written in a coupled manner as

$$\frac{\partial \phi}{\partial x} = \psi(x,t), \quad a < x < b, \tag{7a}$$

$$\frac{\partial^4 \phi}{\partial x^4} = f(x,t,\phi,\phi_t,\psi,\phi_{xx},\psi_{xx}), \quad (x,t) \in \Omega \tag{7b}$$

subject to initial and boundary conditions

$$\phi(x,0) = \phi_0(x), \quad \psi(x,0) = \phi_0'(x), \quad a \le x \le b, \tag{8a}$$

$$\phi(a,t) = g_0(t), \quad \phi(b,t) = g_1(t), \quad \psi(a,t) = h_0(t), \quad \psi(b,t) = h_1(t), \quad t > 0. \tag{8b}$$

Let N be a positive integer, $h = (b-a)/(N+1) > 0$ and $k > 0$ denote the spatial and temporal step sizes, respectively. Define $x_l = a + lh$, $l = 0,1,\ldots,N+1$ and $t_j = jk$, $j = 0,1,\ldots$, then the solution domain Ω is covered by a set of grid points (x_l,t_j). Let $\lambda = (k/h^2) > 0$ be the mesh ratio parameter. Denote Φ_l^j, Ψ_l^j to be the exact solution values of $\phi(x,t)$, $\psi(x,t)$ and ϕ_l^j, ψ_l^j be their approximate solution values, respectively, at the grid point (x_l,t_j).

In order to exemplify the general method employed for constructing the fourth order difference formula for the PDE (1), we first consider the simplest form of the fourth order ordinary differential equation:

$$\frac{d^4\phi}{dx^4} = f(x), \quad a < x < b \tag{9}$$

along with the boundary conditions (3a)–(3b). The Taylor series leads to the following approximations:

$$h^4\left(\frac{d^4\Phi}{dx^4}\right)_l = -12(\Phi_{l-1} - 2\Phi_l + \Phi_{l+1}) + 6h(\Psi_{l+1} - \Psi_{l-1}) - \frac{h^6}{15}\left(\frac{d^6\Phi}{dx^6}\right)_l + O(h^8), \tag{10a}$$

$$h^5\left(\frac{d^5\Phi}{dx^5}\right)_l = -90(\Phi_{l+1}-\Phi_{l-1}) + 30h(\Psi_{l-1}+4\Psi_l+\Psi_{l+1}) + O(h^7), \quad l=1,\ldots,N \tag{10b}$$

Consider

$$h^4(P_0f_l + hP_1f_{x_l} + h^2P_2f_{xx_l}) = P_0h^4\left(\frac{d^4\Phi}{dx^4}\right)_l + P_1h^5\left(\frac{d^5\Phi}{dx^5}\right)_l + h^6P_2\left(\frac{d^6\Phi}{dx^6}\right)_l \tag{11}$$

where $f_l = f(x_l)$, etc. and P_0, P_1, P_2 are the parameters to be determined suitably. Using the approximation (10a) in (11), we obtain

$$\begin{aligned} &h^4(P_0f_l + hP_1f_{x_l} + h^2P_2f_{xx_l}) \\ &= P_0\left[-12(\Phi_{l-1}-2\Phi_l+\Phi_{l+1}) + 6h(\Psi_{l+1}-\Psi_{l-1})\right] + P_1h^5\frac{d^5\Phi}{dx^5} \\ &+ \left(P_2 - \frac{P_0}{15}\right)h^6\left(\frac{d^6\Phi}{dx^6}\right)_l + O(h^8) \end{aligned} \tag{12}$$

Equating the coefficients of h^5 and h^6 to zero in (12), we get $P_1 = 0$ and $P_0 = 15P_2$. Let $P_0 = 15$ and $P_2 = 1$. Using these values of the parameters and the following approximation in (12),

$$f_{xx_l} = \frac{f_{l-1} - 2f_l + f_{l+1}}{h^2} + O(h^2), \tag{13}$$

we obtain the following fourth order approximation for ϕ:

$$\begin{aligned} &-2(\Phi_{l-1}-2\Phi_l+\Phi_{l+1}) + h(\Psi_{l+1}-\Psi_{l-1}) = \frac{h^4}{90}[f_{l-1} + 13f_l + f_{l+1}] + O(h^8), \\ &l = 1,\ldots,N \end{aligned} \tag{14}$$

To obtain fourth order approximation for $\partial\phi/\partial x$, we consider

$$h^4(R_0f_l + hR_1f_{x_l} + h^2R_2f_{xx_l}) = R_0h^4\left(\frac{d^4\Phi}{dx^4}\right)_l + R_1h^5\left(\frac{d^5\Phi}{dx^5}\right)_l + h^6R_2\left(\frac{d^6\Phi}{dx^6}\right)_l \tag{15}$$

where R_0, R_1 and R_2 are the parameters to be found. Using the approximation (10b) in (15), we get

$$\begin{aligned} &h^4(R_0f_l + hR_1f_{x_l} + h^2R_2f_{xx_l}) \\ &= R_0h^4\left(\frac{d^4\Phi}{dx^4}\right)_l + R_1[-90(\Phi_{l+1}-\Phi_{l-1}) + 30h(\Psi_{l-1}+4\Psi_l+\Psi_{l+1})] \\ &+ R_2h^6\left(\frac{d^6\Phi}{dx^6}\right)_l + O(h^7) \end{aligned} \tag{16}$$

Equating the coefficients of h^4 and h^6 to zero in (16), we get $R_0 = 0$, $R_2 = 0$. Since $R_1 \neq 0$, we choose $R_1 = 1$.

Using the approximation

$$f_{x_l} = \frac{f_{l+1} - f_{l-1}}{2h} + O(h^2) \tag{17}$$

in (16), the following discretization for approximating the derivative $\partial\phi/\partial x = \psi$ with $O(h^4)$ accuracy is obtained as

$$-3(\Phi_{l+1} - \Phi_{l-1}) + h(\Psi_{l-1} + 4\Psi_l + \Psi_{l+1}) = \frac{h^4}{60}[f_{l+1} - f_{l-1}] + O(h^7), \quad l = 1, \ldots, N \tag{18}$$

The fundamental schemes (14) and (18) are used to attain the high order difference approximations to the equations (7a)–(7b) which involve both spatial and temporal variables. This is achieved by defining high order approximations to ϕ, ψ, ϕ_t, ϕ_{xx}, ψ_{xx} at each grid point. Using these approximations and following the general schemes (14) and (18) adopted for the ordinary differential equation (9), we derive new difference formula for the PDE (1).

Let

$$\bar{t}_j = t_j + \tau k, \quad 0 < \tau < 1$$

For $r = 0, \pm 1$, we denote

$$\overline{\Phi}^j_{l+r} = \tau\Phi^{j+1}_{l+r} + (1-\tau)\Phi^j_{l+r}, \tag{19a}$$

$$\overline{\Psi}^j_{l+r} = \tau\Psi^{j+1}_{l+r} + (1-\tau)\Psi^j_{l+r}, \tag{19b}$$

$$\overline{\Phi}^j_{t_{l+r}} = (\Phi^{j+1}_{l+r} - \Phi^j_{l+r})/k, \tag{19c}$$

$$\overline{\Phi}^j_{xx_l} = (\overline{\Psi}^j_{l+1} - \overline{\Psi}^j_{l-1})/(2h), \tag{19d}$$

$$\overline{\Psi}^j_{xx_l} = (\overline{\Psi}^j_{l+1} - 2\overline{\Psi}^j_l + \overline{\Psi}^j_{l-1})/h^2. \tag{19e}$$

Using these approximations, we define

$$\begin{aligned}\overline{F}^j_l &= f(x_l, \bar{t}_j, \overline{\Phi}^j_l, \overline{\Phi}^j_{t_l}, \overline{\Psi}^j_l, \overline{\Phi}^j_{xx_l}, \overline{\Psi}^j_{xx_l}) \\ &= F^j_l + kT_0 + O(k^2 + h^2)\end{aligned} \tag{20}$$

where

$$F^j_l = f(x_l, t_j, \Phi^j_l, \Phi^j_{t_l}, \Psi^j_l, \Phi^j_{xx_l}, \Psi^j_{xx_l}),$$

$$T_0 = \tau\left[\left(\frac{\partial f}{\partial t}\right)^j_l + \Phi_{01}\left(\frac{\partial f}{\partial \phi}\right)^j_l + \Phi_{11}\left(\frac{\partial f}{\partial \psi}\right)^j_l + \Phi_{21}\left(\frac{\partial f}{\partial \phi_{xx}}\right)^j_l + \Phi_{31}\left(\frac{\partial f}{\partial \psi_{xx}}\right)^j_l\right] + \frac{\phi_{02}}{2}\left(\frac{\partial f}{\partial \phi_t}\right)^j_l$$

Further, define the approximations for ϕ_{xx} and ψ_{xx} at the neighbouring points $(x_{l\pm1}, \bar{t}_j)$ as

$$\begin{aligned}\overline{\Phi}^j_{xx_{l\pm1}} &= \frac{1}{2h}\left[\pm\overline{\Psi}^j_{l\mp1} \mp 4\overline{\Psi}^j_l \pm 3\overline{\Psi}^j_{l\pm1}\right] \\ &= \Phi^j_{xx_{l\pm1}} + \tau k\Phi_{21} + O(k^2 + h^2),\end{aligned} \tag{21a}$$

$$\begin{aligned}\overline{\Psi}^j_{xx_{l\pm1}} &= \mp\frac{1}{2h^3}\left[21\overline{\Phi}^j_{l\mp1} - 48\overline{\Psi}^j_l + 27\overline{\Phi}^j_{l\pm1}\right] + \frac{1}{2h^2}\left[15\overline{\Psi}^j_{l\pm1} - 9\overline{\Psi}^j_{l\mp1}\right] \\ &= \Psi^j_{xx_{l\pm1}} + \tau k\Phi_{31} + O(k^2 + h^2).\end{aligned} \tag{21b}$$

The functional approximations at $(x_{l\pm1}, \bar{t}_j)$ are defined as

$$\overline{F}^j_{l\pm1} = f(x_{l\pm1}, \bar{t}_j, \overline{\Phi}^j_{l\pm1}, \overline{\Phi}^j_{t_{l\pm1}}, \overline{\Psi}^j_{l\pm1}, \overline{\Phi}^j_{xx_{l\pm1}}, \overline{\Psi}^j_{xx_{l\pm1}})$$
$$= F^j_{l\pm1} + kT_0 + O(\pm hk + k^2 + h^2) \tag{22}$$

For deriving the high order method, we require an $O(k^2 + kh^2 + h^4)$ approximation for $\Phi^j_{xx_l}$. Suppose

$$h^2\overline{\overline{\Phi}}^j_{xx_l} = [a_1\overline{\Phi}^j_{l-1} + a_2\overline{\Phi}^j_l + a_3\overline{\Phi}^j_{l+1}] + h[b_1\overline{\Psi}^j_{l-1} + b_2\overline{\Psi}^j_l + b_3\overline{\Psi}^j_{l+1}] \tag{23}$$

where a_1, a_2, a_3, b_1, b_2 and b_3 are free parameters to be determined. Expanding each term on the right-hand side of (23) in Taylor series about (x_l, t_j) and equating the coefficients up to h^5 to zero, we obtain

$$(a_1, a_2, a_3, b_1, b_2, b_3) = \left(2, -4, 2, \frac{1}{2}, 0, -\frac{1}{2}\right)$$

Thus, we obtain the approximation

$$\overline{\overline{\Phi}}^j_{xx_l} = \frac{2}{h^2}[\overline{\Phi}^j_{l-1} - 2\overline{\Phi}^j_l + \overline{\Phi}^j_{l+1}] - \frac{1}{2h}[\overline{\Psi}^j_{l+1} - \overline{\Psi}^j_{l-1}]$$
$$= \Phi^j_{xx_l} + \tau k\Phi_{21} + O(k^2 + kh^2 + h^4) \tag{24}$$

Similarly, we have

$$\overline{\overline{\Psi}}^j_{xx_l} = \frac{15}{2h^3}[\overline{\Phi}^j_{l+1} - \overline{\Phi}^j_{l-1}] - \frac{3}{2h^2}[\overline{\Psi}^j_{l-1} + 8\overline{\Psi}^j_l + \overline{\Psi}^j_{l+1}]$$
$$= \Psi^j_{xx_l} + \tau k\Phi_{31} + O(k^2 + kh^2 + h^4) \tag{25}$$

Further, an $O(k^2 + kh^2 + h^4)$ approximation for $\Phi^j_{xx_{l+1}}$ is required. For this, let

$$h^2\overline{\overline{\Phi}}^j_{xx_{l+1}} = [c_1\overline{\Phi}^j_{l-1} + c_2\overline{\Phi}^j_l + c_3\overline{\Phi}^j_{l+1}] + h[d_1\overline{\Psi}^j_{l-1} + d_2\overline{\Psi}^j_l + d_3\overline{\Psi}^j_{l+1}] \tag{26}$$

Using the Taylor series expansion about (x_l, t_j) and equating the coefficients up to h^5 to zero, we obtain $(c_1, c_2, c_3, d_1, d_2, d_3) = (-\frac{5}{2}, 8, -\frac{11}{2}, -1, 0, 4)$. Thus, we obtain the approximation

$$\overline{\overline{\Phi}}^j_{xx_{l\pm1}} = -\frac{1}{2h^2}[5\overline{\Phi}^j_{l\mp1} - 16\overline{\Phi}^j_l + 11\overline{\Phi}^j_{l\pm1}] \pm \frac{1}{h}[4\overline{\Psi}^j_{l\pm1} - \overline{\Psi}^j_{l\mp1}]$$
$$= \Phi^j_{xx_{l\pm1}} + \tau k\Phi_{21} + O(\pm hk + k^2 + kh^2 + h^4) \tag{27}$$

Similarly,

$$\overline{\overline{\Psi}}^j_{xx_{l+1}} = \mp\frac{1}{2h^3}[-51\overline{\Phi}^j_{l\mp1} - 48\overline{\Phi}^j_l + 99\overline{\Phi}^j_{l\pm1}] + \frac{1}{2h^2}[15\overline{\Psi}^j_{l\mp1} + 96\overline{\Psi}^j_l + 39\overline{\Psi}^j_{l\pm1}]$$
$$= \Psi^j_{xx_{l\pm1}} + \tau k\Phi_{31} + O(\pm hk + k^2 + kh^2 + h^4) \tag{28}$$

Now, we define

$$\overline{\overline{F}}_l^j = f(x_l, \bar{t}_j, \overline{\Phi}_l^j, \overline{\Phi}_{t_l}^j, \overline{\Psi}_l^j, \overline{\overline{\Phi}}_{xx_l}^j, \overline{\overline{\Psi}}_{xx_l}^j), \tag{29a}$$

$$\overline{\overline{F}}_{l\pm1}^j = f(x_{l\pm1}, \bar{t}_j, \overline{\Phi}_{l\pm1}^j, \overline{\Phi}_{t_{l\pm1}}^j, \overline{\Psi}_{l\pm1}^j, \overline{\overline{\Phi}}_{xx_{l\pm1}}^j, \overline{\overline{\Psi}}_{xx_{l\pm1}}^j) \tag{29b}$$

Then an $O(k^2 + kh^2 + h^4)$ finite difference method for the differential equation (1) is given by

$$-2(\overline{\Phi}_{l-1}^j - 2\overline{\Phi}_l^j + \overline{\Phi}_{l+1}^j) + h(\overline{\Psi}_{l+1}^j - \overline{\Psi}_{l-1}^j) = \frac{h^4}{90}[\overline{F}_{l-1}^j + 13\overline{\overline{F}}_l^j + \overline{\overline{F}}_{l+1}^j] + \overline{T}_l^{j(1)},$$
$$l = 1, \dots, N, \quad j = 0, 1, \dots \tag{30}$$

and the corresponding approximation for $\partial\phi/\partial x$ can be written as

$$-3(\overline{\Phi}_{l+1}^j - \overline{\Phi}_{l-1}^j) + h(\overline{\Psi}_{l+1}^j + 4\overline{\Psi}_l^j + \overline{\Psi}_{l+1}^j) = \frac{h^4}{60}[\overline{F}_{l+1}^j - \overline{F}_{l-1}^j] + \overline{T}_l^{j(2)},$$
$$l = 1, \dots, N, \quad j = 0, 1, \dots \tag{31}$$

With the help of approximations (24)–(28), from Equations (29a)–(29b), we obtain

$$\overline{\overline{F}}_l^j = F_l^j + kT_0 + O(k^2 + kh^2 + h^4) \tag{32a}$$

$$\overline{\overline{F}}_{l\pm1}^j = F_{l\pm1}^j + kT_0 + O(\pm hk + k^2 + kh^2 + h^4) \tag{32b}$$

From Equations (32a)–(32b), we have

$$\overline{\overline{F}}_{l-1}^j + 13\overline{\overline{F}}_l^j + \overline{\overline{F}}_{l+1}^j = 15F_l^j + h^2\left(\frac{\partial^2 f}{\partial x^2}\right)_l^j + 15kT_0 + O(k^2 + kh^2 + h^4) \tag{33}$$

With the help of relation (33) and the approximations (19a)–(19b), the local truncation error $\overline{T}_l^{j(1)}$ associated with the difference formula (30) is obtained as

$$\overline{T}_l^{j(1)} = -\frac{kh^4}{6}\left(\tau - \frac{1}{2}\right)\Phi_{02}\left(\frac{\partial f}{\partial \phi_t}\right)_l^j + O(k^2h^4 + kh^6 + h^8) \tag{34}$$

For the proposed difference scheme (30) to be of $O(k^2 + kh^2 + h^4)$, the coefficient of kh^4 in (34) must be zero. Consequently, we obtain $\tau = 1/2$ and the local truncation error associated with (30) becomes $\overline{T}_l^{j(1)} = O(k^2h^4 + kh^6 + h^8)$.

Similarly, it is seen that $\overline{T}_l^{j(2)} = O(k^2h^3 + kh^5 + h^7)$ and thus the difference scheme (31) is an $O(k^2 + kh^2 + h^4)$ approximation for the derivative $\partial\phi/\partial x = \psi$.

The matrices represented by the difference formulas (30)–(31) are block tri-diagonal for which we have used block iterative methods (see [9,11]). It is noted that the difference method (30)–(31) has fourth order accuracy in space for a fixed value of the mesh ratio parameter $\lambda = k/h^2$.

3. Stability consideration

We discuss the stability of the derived scheme using the von Neumann stability analysis for the following 1D unsteady biharmonic problem:

$$\frac{\partial^4\phi}{\partial x^4} = -\frac{\partial\phi}{\partial t} + f(x,t), \quad 0 < x < 1, \quad t > 0 \tag{35}$$

The proposed difference method (30)–(31) applied to Equation (35) can be written as

$$\begin{aligned}
&(\phi_{l-1}^{j+1} + 13\phi_l^{j+1} + \phi_{l+1}^{j+1}) - 90\,p(\phi_{l-1}^{j+1} - 2\phi_l^{j+1} + \phi_{l+1}^{j+1}) + 45\,ph(\psi_{l+1}^{j+1} - \psi_{l-1}^{j+1})\\
&\quad = (\phi_{l-1}^{j} + 13\phi_l^{j} + \phi_{l+1}^{j}) + 90\,p(\phi_{l-1}^{j} - 2\phi_l^{j} + \phi_{l+1}^{j}) - 45\,ph(\psi_{l+1}^{j} - \psi_{l-1}^{j}) + \Sigma f
\end{aligned} \tag{36a}$$

$$\begin{aligned}
&(1-90\,p)(\phi_{l+1}^{j+1} - \phi_{l-1}^{j+1}) + 30\,ph(\psi_{l-1}^{j+1} + 4\psi_l^{j+1} + \psi_{l+1}^{j+1})\\
&\quad = (1+90\,p)(\phi_{l+1}^{j} - \phi_{l-1}^{j}) - 30\,ph(\psi_{l-1}^{j} + 4\psi_l^{j} + \psi_{l+1}^{j}) + \Sigma f_1,\\
&l = 1,\ldots,N, \quad j = 0,1,\ldots
\end{aligned} \tag{36b}$$

where $p = k/h^4$, $\Sigma f = k[\bar{f}_{l-1}^j + 13\bar{f}_l^j + \bar{f}_{l+1}^j]$ and $\Sigma f_1 = k[\bar{f}_{l+1}^j - \bar{f}_{l-1}^j]$.

To apply the von Neumann method, we assume that the solutions are given by

$$\phi_l^j = \xi^j e^{i\beta l},$$
$$\psi_l^j = \eta^j e^{i\beta l},$$

for $i = \sqrt{-1}$, ξ, η being the amplification factors and β being the phase angle. Using these in the homogenous part of the scheme (36a)–(36b) will lead us to the following system:

$$\begin{bmatrix} a & b \\ c & d \end{bmatrix} \begin{bmatrix} \xi \\ \eta \end{bmatrix}^{j+1} = \begin{bmatrix} r & -b \\ s & -d \end{bmatrix} \begin{bmatrix} \xi \\ \eta \end{bmatrix}^{j} \tag{37}$$

where

$$\begin{aligned}
&a = 15 - 4\sin^2\frac{\beta}{2} + 360\,p\sin^2\frac{\beta}{2}, \quad b = 180\,ph\sin\frac{\beta}{2}\cos\frac{\beta}{2}i,\\
&c = 4i(1-90\,p)\sin\frac{\beta}{2}\cos\frac{\beta}{2}, \quad d = 60\,ph(3 - 2\sin^2\frac{\beta}{2}),\\
&r = 15 - 4\sin^2\frac{\beta}{2} - 360\,p\sin^2\frac{\beta}{2}, \quad s = 4i(1+90\,p)\sin\frac{\beta}{2}\cos\frac{\beta}{2}.
\end{aligned}$$

The system (37) can be written in a matrix-vector form as

$$\begin{bmatrix} \xi \\ \eta \end{bmatrix}^{j+1} = \boldsymbol{H} \begin{bmatrix} \xi \\ \eta \end{bmatrix}^{j}, \tag{38}$$

where the amplification matrix is given by

$$\boldsymbol{H} = \begin{bmatrix} a & b \\ c & d \end{bmatrix}^{-1} \begin{bmatrix} r & -b \\ s & -d \end{bmatrix}$$

The von Neumann necessary condition for the stability of the system (38) is that the maximum modulus of the eigenvalues of the amplification matrix $\boldsymbol{H}$ are to be less than or equal to one. By direct calculation, the eigenvalues of the matrix $\boldsymbol{H}$ are given by

$$\rho_1 = -1, \quad \rho_2 = \frac{rd - sb}{ad - bc}$$

Simplifying, we get

$$\rho_2 = \frac{45 - 30\sin^2\frac{\beta}{2} - 4\sin^4\frac{\beta}{2} - 360\,p\sin^4\frac{\beta}{2}}{45 - 30\sin^2\frac{\beta}{2} - 4\sin^4\frac{\beta}{2} + 360\,p\sin^4\frac{\beta}{2}}$$

Since $\min(45 - 30\sin^2\beta/2 - 4\sin^4\beta/2) = 11 > 0$, for $\beta \in [-\pi, \pi]$, it is observed that $|\rho_1|$, $|\rho_2| \le 1$ for all phase angles β. Thus, the derived scheme applied to the linear equation (35) is unconditionally stable.

4. Application to the linear singular equation

Consider the following class of 1D unsteady biharmonic problem:

$$\nabla^4\phi + \frac{\partial\phi}{\partial t} \equiv \left(\frac{\partial^2}{\partial r^2} + d(r)\frac{\partial}{\partial r}\right)^2 \phi + \frac{\partial\phi}{\partial t} = g(r,t),$$

where $(r,t) \in \Lambda \equiv \{(r,t)|\, 0 < r < 1,\ t > 0\}$, or equivalently,

$$\frac{\partial^4\phi}{\partial r^4} = A(r)\frac{\partial^3\phi}{\partial r^3} + B(r)\frac{\partial^2\phi}{\partial r^2} + C(r)\frac{\partial\phi}{\partial r} - \frac{\partial\phi}{\partial t} + g(r,t), \quad (r,t) \in \Lambda, \tag{39}$$

where

$$A(r) = -2d(r), \quad B(r) = -\left(2d'(r) + d^2(r)\right), \quad C(r) = -\left(d''(r) + d(r)d'(r)\right).$$

Replacing the variable x by r and applying the difference formula (30)–(31) to Equation (39), we obtain numerical approximation of $O(k^2 + kh^2 + h^4)$ as

$$\begin{aligned} &-2(\bar{\phi}^j_{l-1} - 2\bar{\phi}^j_l + \bar{\phi}^j_{l+1}) + h(\bar{\psi}^j_{l+1} - \bar{\psi}^j_{l+1}) \\ &= \frac{h^4}{90}\Big[A_{l-1}\bar{\bar{\psi}}^j_{rr_{l-1}} + B_{l-1}\bar{\bar{\phi}}^j_{rr_{l-1}} + C_{l-1}\bar{\psi}^j_{l-1} - \bar{\phi}^j_{t_{l-1}} + \bar{g}^j_{l-1} \\ &\quad + 13\left(A_l\bar{\bar{\psi}}^j_{rr_l} + B_l\bar{\bar{\phi}}^j_{rr_l} + C_l\bar{\psi}^j_l - \bar{\phi}^j_{t_l} + \bar{g}^j_l\right) + A_{l+1}\bar{\bar{\psi}}^j_{rr_{l+1}} \\ &\quad + B_{l+1}\bar{\bar{\phi}}^j_{rr_{l+1}} + C_{l+1}\bar{\psi}^j_{l+1} - \bar{\phi}^j_{t_{l+1}} + \bar{g}^j_{l+1}\Big] \end{aligned} \tag{40a}$$

$$\begin{aligned} &-3(\bar{\phi}^j_{l+1} - \bar{\phi}^j_{l-1}) + h(\bar{\psi}^j_{l-1} + 4\bar{\psi}^j_l + \bar{\Psi}^j_{l+1}) \\ &= \frac{h^4}{60}\Big[A_{l+1}\bar{\psi}^j_{rr_{l+1}} + B_{l+1}\bar{\phi}^j_{rr_{l+1}} + C_{l+1}\bar{\psi}^j_{l+1} - \bar{\phi}^j_{t_{l+1}} + \bar{g}^j_{l+1} \\ &\quad - A_{l-1}\bar{\psi}^j_{rr_{l-1}} - B_{l-1}\bar{\phi}^j_{rr_{l-1}} - C_{l-1}\bar{\psi}^j_{l-1} + \bar{\phi}^j_{t_{l-1}} - \bar{g}^j_{l-1}\Big], \\ &\quad l = 1, \ldots, N,\ j = 0, 1, \ldots \end{aligned} \tag{40b}$$

If the coefficient $d(r)$ includes the singular terms like $1/r$, $1/r^2, \ldots$, then the scheme (40a)–(40b) fails to compute the solution at $l = 1$. For instance, when $d(r) = \alpha/r$, then

$\nabla^2 \equiv \partial^2/\partial r^2 + \alpha/r\partial/\partial r$ represents the one-dimensional Laplacian operator in cylindrical and spherical coordinates, for $\alpha = 1$ and 2, respectively. Thus, in this case the one-space dimensional unsteady biharmonic equation in cylindrical and spherical coordinates is Equation (39) for

$$A(r) = \frac{-2\alpha}{r}, \quad B(r) = \frac{\alpha(2-\alpha)}{r^2}, \quad C(r) = \frac{\alpha(\alpha-2)}{r^3}.$$

Although the difference scheme (40a)–(40b) is of $O(k^2 + kh^2 + h^4)$ but in this case it involve the terms A_{l-1}, B_{l-1}, C_{l-1}, $\overline{g}^j_{l-1}$, all of which contain the term $1/r_{l-1}$ giving rise to singularity at $l = 1$ since $r_0 = 0$. It is for this reason that the proposed method is not directly applicable to singular equations in the region $0 < r < 1$, i.e. in the vicinity of singularity. We overcome this shortcoming by using the following approximations:

$$A_{l\pm1} = A_{00} \pm hA_{10} + \frac{h^2}{2}A_{20} + O(h^3), \tag{41a}$$

$$B_{l\pm1} = B_{00} \pm hB_{10} + \frac{h^2}{2}B_{20} + O(h^3), \tag{41b}$$

$$C_{l\pm1} = C_{00} \pm hC_{10} + \frac{h^2}{2}C_{20} + O(h^3), \tag{41c}$$

$$\overline{g}^j_{l\pm1} = \overline{g}^j_l \pm h\overline{g}^j_{x_l} + \frac{h^2}{2}\overline{g}^j_{xx_l} + O(h^3), \tag{41d}$$

where $\overline{g}^j_l = g(x_l, \overline{t}_j)$, $\overline{g}^j_{x_l} = g_x(x_l, \overline{t}_j)$, etc.

Using the approximations (41a)–(41d) in the difference scheme (40a)–(40b) and neglecting higher order terms, we obtain following modified difference approximations in the operator compact form:

$$\begin{aligned}
& p\left[-180 + h^2\left(24A_{10} - 18B_{00} + 4h^2B_{20}\right)\right]\delta_x^2\overline{\phi}^j_l \\
&\quad + \frac{ph}{2}\left[-45A_{00} + 75h^2A_{20} + 6h^2B_{10}\right](2\mu_x\delta_x)\overline{\phi}^j_l \\
&\quad + ph^2\left[45A_{00} - h^2\left(75A_{20} + 6B_{10} + 15C_{00} + h^2C_{20}\right)\right]\overline{\psi}^j_l \\
&\quad + \frac{ph^2}{2}\left[-15A_{00} - h^2\left(27A_{20} + 6B_{10} + 2C_{00}\right)\right]\delta_x^2\overline{\psi}^j_l \\
&\quad + \frac{ph}{2}\left[180 - h^2\left(24A_{10} - 3B_{00} + 5h^2B_{20} + 2h^2C_{10}\right)\right](2\mu_x\delta_x)\overline{\psi}^j_l \\
&\quad + \left(\phi^{j+1}_{l-1} + 13\phi^{j+1}_l + \phi^{j+1}_{l+1}\right) \\
&\quad\quad = \left(\phi^j_{l-1} + 13\phi^j_l + \phi^j_{l+1}\right) + k\left[15\overline{g}^j_l + h^2\overline{g}^j_{xx_l}\right],
\end{aligned} \tag{42a}$$

$$ph\left[24A_{00}\right]\delta_x^2\overline{\phi}^j_l + p\left[-180 + 3h^2A_{10}\right](2\mu_x\delta_x)\overline{\phi}^j_l + ph\left[360 - h^2(6A_{10} + 2h^2C_{10})\right]\overline{\psi}^j_l$$

$$ph\left[60-h^2(2B_{00}+3A_{10})\right]\delta_x^2\overline{\psi}_l^j+ph^2\left[-12A_{00}-h^2(B_{10}+C_{00})\right]$$
$$\times(2\mu_x\delta_x)\overline{\psi}_l^j+(2\mu_x\delta_x)\phi_l^{j+1}$$
$$=k\left[2h\overline{g}_{x_l}^j\right]+(2\mu_x\delta_x)\phi_l^j,\quad l=1,\ldots,N,\quad j=0,1,\ldots \tag{42b}$$

where $p=k/h^4$, $\delta_x\phi_l=\phi_{l+(1/2)}-\phi_{l-(1/2)}$ and $\mu_x\phi_l=1/2(\phi_{l+(1/2)}+\phi_{l-(1/2)})$ denote the central and average difference operators with respect to the x-direction, respectively.

It is noted that the difference method (42a)–(42b) is a two-level implicit method of $O(k^2+kh^2+h^4)$ which does not include the term $1/r_{l-1}$, thus can be easily solved for $l=1,\ldots,N$ in the region $[0<r<1]\times[t>0]$. The resulting system of tri-diagonal matrices can be solved using block iterative methods (see Kelly [11]).

5. Numerical examples

In this section, the proposed difference scheme is tested on several problems of physical significance to verify the theoretical findings. The initial and boundary conditions correspond to the data from exact solution. At each interior grid point, the resulting matrix system has two unknowns ϕ and $\partial\phi/\partial x\equiv\psi$ which are solved using suitable block iterative methods. We have solved the nonlinear equations by Newton's nonlinear block Gauss-Seidel iteration method (see Hageman and Young [9], Kelly [11]) while linear equations of these kind have been solved using the block Gauss-Seidel iteration method. The initial vector $(0,0)$ is used in all the cases and the iterations were stopped when the absolute error tolerance $|\phi^{(k+1)}-\phi^{(k)}|+|\psi^{(k+1)}-\psi^{(k)}|\le 2\times10^{-10}$ was attained.

Example 1: [12,22] Consider the GKS equation (4) for $\alpha=\gamma=1$ and $\beta=12/\sqrt{47}$. The exact solution is given by

$$\phi(x,t)=-\frac{396.8}{47\sqrt{47}}+\frac{15}{47\sqrt{47}}\left[3\tanh\theta-3\tanh^2\theta+\tanh^3\theta\right],$$

with $\theta=(1/2\sqrt{47})x+0.1t$. The computational domain is taken as $[-1,1]$. The L_∞ errors by applying the proposed method for $h=1/8$ and same time step $k=0.05$ as taken in [22] corresponding to different time levels are reported in Table 1 and compared with the results proposed in [12,22]. It should be pointed out that with spatial step size $h=1/8$, the proposed method is more accurate than [12,22], where 9 collocating points were taken so that the dimension of the arising system is 9×9 in [22] while for the best results in [12], the dimension of the system is 11×11 at each level of time. Figure 1 shows the exact and numerical solutions at $t=1$ for $h=1/8$ and $k=0.05$.

Example 2: [12,22] We show an accuracy test for the GKS equation (4) with $\alpha=\gamma=1$ and $\beta=16/\sqrt{73}$ on the interval $[-1,1]$. The exact solution is given by

$$\phi(x,t)=-\frac{1005.8}{73\sqrt{73}}+\frac{15}{73\sqrt{73}}\left[5\tanh\theta-4\tanh^2\theta+\tanh^3\theta\right],$$

with $\theta=(1/2\sqrt{73})x+0.1t$. Table 2 gives the comparison between the L_∞ errors in the computed solution by the proposed method for $h=1/8$ and $k=0.05$ at different values of

Table 1. Comparison of L_∞ errors with earlier schemes for $h = 1/8$ and $k = 0.05$ at different times, Example 1

t	Proposed method	Method [22]	Method [12]
0.2	1.1746e−011	2.41e−010	2.38e−007
0.4	1.0980e−011	2.38e−010	2.38e−007
0.6	1.3775e−011	6.36e−010	2.38e−007
0.8	1.8141e−011	1.05e−009	1.19e−007
1.0	2.2219e−011	5.95e−010	2.38e−007
3.0	9.6846e−011	3.01e−009	–
5.0	1.0378e−010	3.05e−009	–
10	3.7657e−011	6.88e−010	–

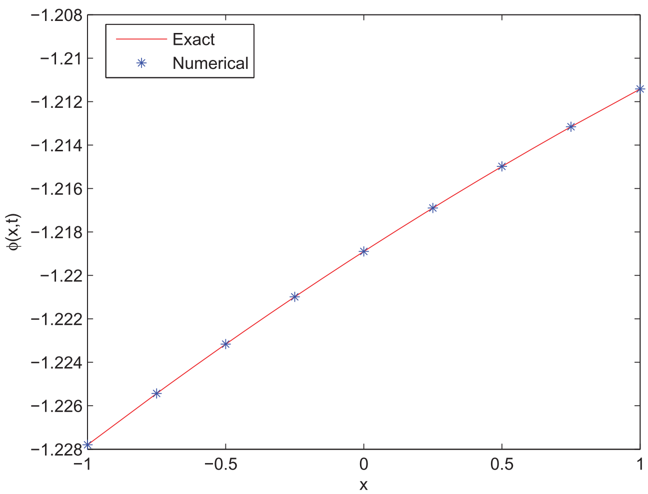

Figure 1. Plot of exact-numerical solution at $t = 1$ with $k = 0.05$ and $h = 1/8$, Example 1

Table 2. Comparison of L_∞ errors with earlier schemes for $h = 1/8$ and $k = 0.05$ at different times, Example 2.

t	Proposed method	Method [22]	Method [12]
0.2	1.9195e−011	1.25e−009	2.38e−007
0.4	1.5246e−011	9.76e−010	1.19e−007
0.6	1.1641e−011	7.06e−010	1.19e−007
0.8	8.5720e−012	4.44e−010	2.38e−007
1.0	6.1005e−012	1.94e−010	2.38e−007
3.0	6.2855e−011	1.64e−009	–
5.0	7.7362e−011	2.08e−009	–
10	4.1989e−011	7.37e−010	–

time with that given in [12,22]. The present method uses only 9 grid points at each time step while the accuracy is more high as compared with the existing methods [12,22]. Figure 2 provides the analytical solution and the computational simulation at $t = 5$ for $h = 1/8$ and $k = 0.05$.

Example 3: [12,15] In the below example, the GKS equation (4) represented by $\alpha = \gamma = 1$ and $\beta = 4$ has been considered. The exact solution is

$$\phi(x, t) = 9 + 2c + 15 \tanh\theta - 15 \tanh^2\theta - 15 \tanh^3\theta$$

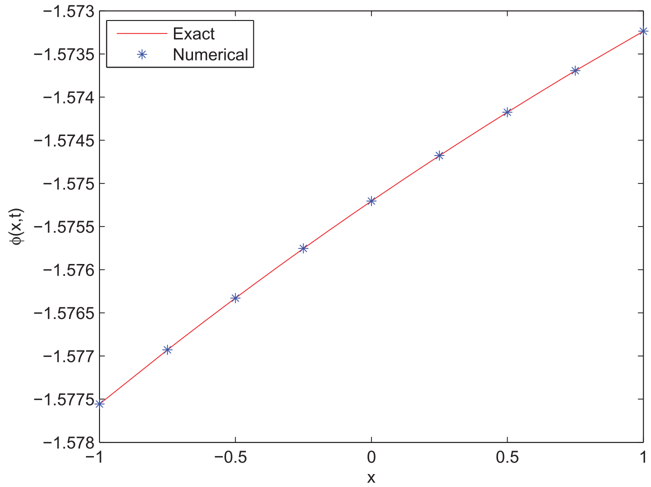

Figure 2. Plot of exact-numerical solution at $t = 5$ with $k = 0.05$ and $h = 1/8$, Example 2

Table 3. Comparison of L_∞ and L_2 errors for $c = 1$ at $t = 1$ for different values of h and k, Example 3.

k	Proposed method	Method [15]	Proposed method	Method [15]	Proposed method	Method [15]	Proposed method	Method[15]
	$h = 1/16$ L_∞	$(J = 4)$ L_∞	$h = 1/16$ L_2	$(J = 4)$ L_2	$h = 1/32$ L_∞	$(J = 5)$ L_∞	$h = 1/32$ L_2	$(J = 5)$ L_2
0.1	1.1333e−003	7.3e−003	5.9247e−004	6.5e−003	1.0080e−003	4.4e−003	5.2492e−004	3.7e−003
0.01	2.1124e−005	6.1e−003	1.2896e−005	5.7e−003	1.2077e−005	3.3e−005	6.5606e−006	2.6e−005
0.001	1.2057e−005	1.0e−004	8.0184e−006	8.4e−005	8.1647e−007	2.8e−006	5.3809e−007	1.5e−006

Table 4. Comparison of L_∞ errors for $h = 1/32$ and $k = 0.05$ at $t = 1$ for different values of c with [12,15], Example 3.

c	Proposed method	Method [15]	Method [12]
0.1	1.2972e−005	7.7e−007	2.6e−004
0.01	8.5765e−007	1.8e−006	3.2e−005
0.001	9.4673e−007	1.6e−006	3.2e−005

with $\theta = -(1/2)x + ct$. The computation domain is taken as $[-1, 1]$. The L_∞ and L_2 errors obtained by the proposed method for $c = 1$ at time $t = 1$ for different values of h and k are compared with the results of [15] in Table 3. Also, the L_∞ errors for different values of c are presented in Table 4 at time $t = 1$ for $k = 0.05$, $h = 1/32$ and compared with the methods proposed in [12,15]. Figure 3(a) compares the analytical solution against the numerical approximation computed through the proposed method for $c = 1$ at $t = 2$ with $h = 1/16$, $k = 0.01$ and Figure 3(b) shows the exact-numerical solutions for $c = 0.001$ at $t = 1$ with $h = 1/32$ and $k = 0.05$.

Example 4: [15] We conduct an accuracy test for the KS equation (5) for $\alpha = 2$ and $\gamma = 1$ on the interval $[-1, 1]$. The exact solution is given by

$$\phi(x,t) = -\frac{1}{K} + \frac{60}{19}K(-38\gamma K^2 + \alpha)\tanh\theta + 120\gamma K^3 \tanh^3\theta$$

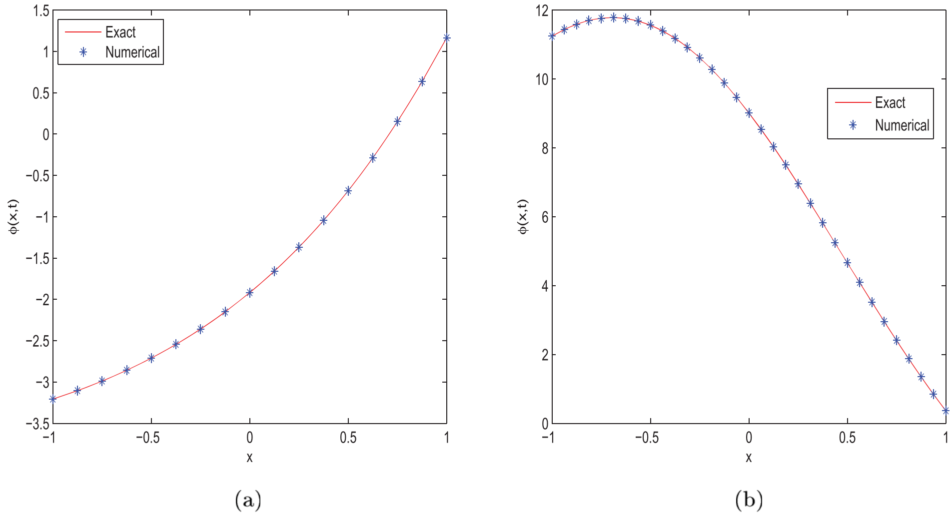

Figure 3. Plots of exact-numerical solutions, Example 3. (a) $c = 1$, $t = 2$ with $h = 1/16$, $k = 0.01$ and (b) $c = 0.001$, $t = 1$ with $h = 1/32$, $k = 0.05$.

with $\theta = Kx + t$ and $K = (1/2)\sqrt{11\alpha/19\gamma}$. Table 5 gives the comparison of L_∞ and L_2 errors of the computed results with that given in [15] at time $t = 1$ for different values of h and k. The graph of exact-numerical solutions at $t = 1$ with $h = 1/16$ and $k = 0.1$ is plotted in Figure 4.

Example 5: [15,16] Consider the KS equation (5) which represents the simplest nonlinear PDE demonstrating chaotic behaviour over a finite spatial domain with the Gaussian initial condition

$$\phi(x, 0) = \exp(-x^2) \tag{43}$$

and the boundary conditions

$$\phi(a, t) = 0, \quad \phi(b, t) = 0, \quad \frac{\partial \phi}{\partial x}(a, t) = 0, \quad \frac{\partial \phi}{\partial x}(b, t) = 0 \tag{44}$$

The computational domain is taken as $[a, b] = [-30, 30]$ with $k = 0.01$ and number of partitions as 100. In Figure 5(a,b), the computed results are displayed showing complete chaotic behaviour at $t = 5$ and $t = 20$, respectively. We can observe that the results present

Table 5. Comparison of L_∞ and L_2 errors at $t = 1$ for different values of h and k, Example 4.

k	Proposed method	Method [15]	Proposed method	Method [15]	Proposed Method	Method [15]	Proposed method	Method [15]
	$h = 1/16$ L_∞	$(J = 4)$ L_∞	$h = 1/16$ L_2	$(J = 4)$ L_2	$h = 1/32$ L_∞	$(J = 5)$ L_∞	$h = 1/32$ L_2	$(J = 5)$ L_2
0.1	1.1658e−004	1.3e−003	7.4861e−005	1.2e−003	2.0355e−004	1.7e−003	1.2777e−004	1.5e−003
0.01	1.4081e−005	4.2e−004	9.5622e−006	3.7e−004	2.7840e−006	9.0e−005	1.6379e−006	8.0e−005
0.001	9.2622e−006	9.7e−005	1.4869e−005	9.1e−005	3.0516e−006	6.2e−006	1.8069e−006	5.5e−006

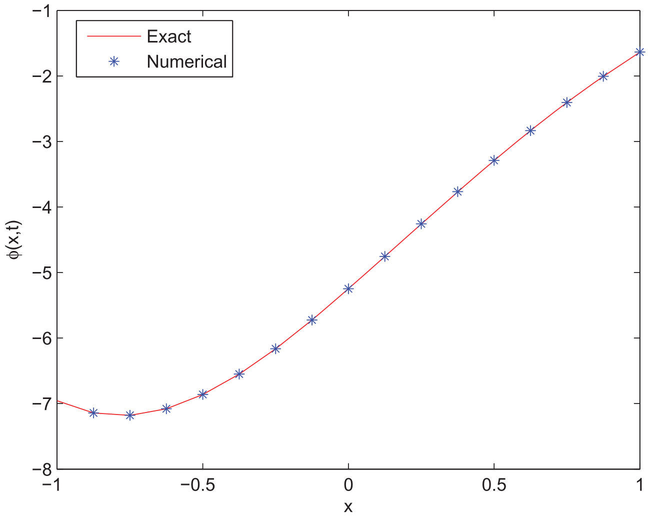

Figure 4. Plot of exact-numerical solution at $t = 1$ with $k = 0.1$ and $h = 1/16$, Example 4.

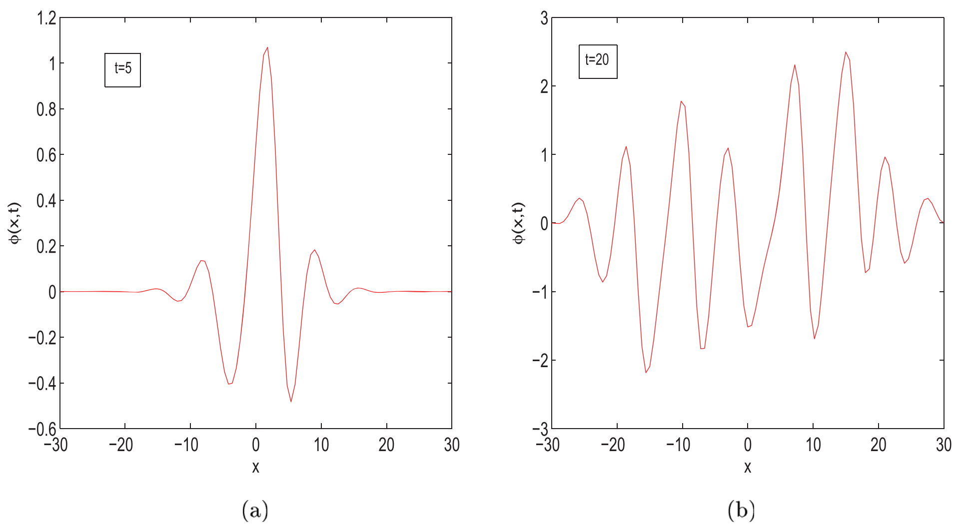

Figure 5. The chaotic solution of the KS equation (5) for $\alpha = 2$ and $\gamma = 1$ with the Gaussian initial condition (43) at $t = 5$ and $t = 20$, Example 5. (a) Numerical solution at $t = 5$ and (b) Numerical solution at $t = 20$.

the same characteristics as in [16] and are numerically convergent for the chaotic behaviour too.

Example 6: Consider the linear singular equation (39) for $d(r) = \alpha/r$, $\alpha = 1, 2$ with the exact solution $\phi(r, t) = e^{-t} r^4 \sin r$. We employ the difference scheme (42a)–(42b) to compute the solution and display the L_∞ errors in ϕ and $\partial\phi/\partial r$ vs. N with 9 to 33 nodal points for $\lambda = 1.6$ in Figure 6 for $\alpha = 1, 2$ at $t = 1$ illustrating fourth order accurate results for a fixed value of mesh ratio parameter.

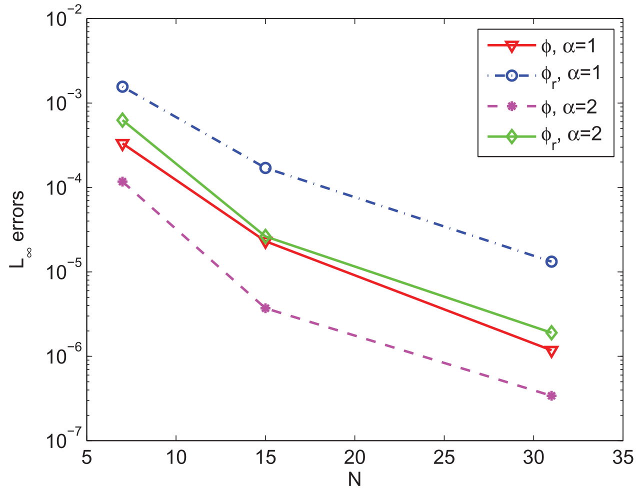

Figure 6. L_∞ errors versus N with $\lambda = 1.6$ at $t = 1$ for $\alpha = 1, 2$, Example 6.

Table 6. L_∞ errors at $t = 1$ for different values of γ with $\lambda = (k/h^2) = 1.6$, Example 7.

h		L_∞ $\gamma = 0.1$	Order $\gamma = 0.1$	L_∞ $\gamma = 0.01$	Order $\gamma = 0.01$	L_∞ $\gamma = 0.001$	Order $\gamma = 0.001$
1/8	ϕ	1.7646e−005	–	3.0730e−005	–	4.5315e−005	–
	ϕ_x	4.8192e−005	–	6.9878e−005	–	6.4717e−005	–
1/16	ϕ	1.1527e−006	3.9363	2.0130e−006	3.9322	2.7491e−006	4.0430
	ϕ_x	3.4162e−006	3.8183	5.7280e−006	3.6087	4.0259e−006	4.0068
1/32	ϕ	7.1483e−008	4.0113	1.2713e−007	3.9850	1.6854e−007	4.0278
	ϕ_x	2.1865e−007	3.9657	3.8537e−007	3.8937	2.5184e−007	3.9987

Example 7: Consider the following non-homogenous EFK equation:

$$\frac{\partial \phi}{\partial t} + \gamma \frac{\partial^4 \phi}{\partial x^4} - \frac{\partial^2 \phi}{\partial x^2} + f(\phi) = g(x,t), \quad 0 < x < 1, \quad t > 0 \tag{45}$$

where $f(\phi) = \phi^3 - \phi$. Here,

$$g(x,t) = \left(\gamma\pi^4 + \pi^2 + e^{-2t}\sin^2(\pi x) - 2\right) e^{-t}\sin(\pi x).$$

The exact solution of the above equation is $\phi(x,t) = e^{-t}\sin(\pi x)$. The L_∞ errors and order of convergence using the proposed method are tabulated in Table 6 at $t = 1$ for various values of γ for $h = 1/8,\ 1/16,\ 1/32$ and $\lambda = 1.6$. For every spatial mesh length h, the corresponding time step is selected as $k \propto h^2$. With this choice of time step, the proposed method has accuracy of fourth order in space as illustrated in Table 6.

6. Concluding remarks

The conventional approach of splitting the fourth order PDE into coupled second order equations is not possible with ϕ and $\partial\phi/\partial x$ prescribed at the boundary and hence deriving compact finite difference schemes is difficult in this case. Using a combination of values of the solution $\phi(x,t)$ and its first order space derivative $\partial\phi/\partial x$, we develop a high order two-level implicit difference formula for the unsteady biharmonic equation in the one-space variable with Dirichlet and Neumann boundary conditions. The present approach is advantageous since it is defined on a three-point compact stencil and no fictitious points outside the solution domain are needed to handle the boundary conditions. The value of $\partial\phi/\partial x$ is already calculated and available at all grid points and it is not required to be further approximated from the calculated values of the solution. We examine the stability of the proposed scheme using the von Neumann method and it is shown to be unconditionally stable for a model linear problem. The proposed numerical method is also applicable to the class of linear singular problems by incorporating suitable approximations and produces stable solutions even in the vicinity of the singularity. The employed method works well for a large class of linear and nonlinear problems including the more complex fourth order equations like the GKS equation and EFK equation. A comparative study is done with results available in the literature and it is found that the current approach produces more accurate results in comparison with those already proposed in [12,15,22] using less grid points at each level of time. The presented method is relatively straightforward and without using any transformation or the linearization technique it gives considerably accurate solutions with sparser grid points and fewer time steps, thus reducing the complexity and computational cost. The calculated results show that the method provides fourth order convergent results for a fixed mesh ratio parameter λ for the EFK equation. We are presently working to extend this approach to the two-dimensional case to solve higher dimensional time-dependent problems occurring in several fields of science and engineering.

Disclosure statement

No potential conflict of interest was reported by the author(s).

ORCID

R.K. Mohanty http://orcid.org/0000-0001-6832-1239

References

[1] G.D. Akrivis, *Finite difference discretization of the Kuramoto-Sivashinsky equation*, Numer. Math. 63 (1992), pp. 1–11.
[2] G. Akrivis and S. Yiorgos-Sokratis, *Implicit-explicit BDF methods for the Kuramoto-Sivashinsky equation*, Appl. Numer. Math. 51 (2004), pp. 151–169.
[3] D.G. Aronson and H.F. Weinberger, *Multidimensional nonlinear diffusion arising in population genetics*, Adv. Math. 30 (1978), pp. 33–76.
[4] P. Danumjaya, *Finite element methods for one dimensional fourth order semilinear partial differential equation*, Int. J. Appl. Comput. Math. 2 (2016), pp. 395–410.
[5] G.T. Dee and W. Van Saarloos, *Bistable systems with propagating fronts leading to pattern formation*, Phys. Rev. Lett. 60 (1988), pp. 2641–2644.
[6] L.J.T. Doss and A.P. Nandini, *An H^1-Galerkin mixed finite element method for the extended Fisher-Kolmogorov equation*, Int. J. Numer. Anal. Model. Ser. B 3 (2012), pp. 460–485.
[7] E. Fan, *Extended tanh-function method and its applications to nonlinear equations*, Phys. Lett. A277 (2000), pp. 212–218.
[8] I.A. Ganaie, S. Arora and V.K. Kukreja, *Cubic Hermite collocation solution of Kuramoto-Sivashinsky equation*, Int. J. Comput. Math. 93 (2016), pp. 223–235.
[9] L.A. Hageman and D.M. Young, *Applied Iterative Methods*, Dover Publication, New York, 2004.

[10] A.P. Hooper and R. Grimshaw, *Nonlinear instability at the interface between two viscous fluids*, Phys. Fluids 28 (1985), pp. 37–45.
[11] C.T. Kelly, *Iterative Methods for Linear and Non-linear Equations*, SIAM Publications, Philadelphia, 1995.
[12] A.H. Khater and R.S. Temsah, *Numerical solutions of the generalized Kuramoto-Sivashinsky equation by Chebyshev spectral collocation methods*, Comput. Math. Appl. 56 (2008), pp. 1465–1472.
[13] Y. Kuramoto and T. Tsuzuki, *Persistent propagation of concentration waves in dissipative media far from thermal equilibrium*, Prog. Theor. Phys. 55 (1976), pp. 356–369.
[14] H. Lai and C. Ma, *Lattice Boltzmann method for the generalized Kuramoto-Sivashinsky equation*, Physica A 388 (2009), pp. 1405–1412.
[15] M. Lakestani and M. Dehghan, *Numerical solutions of the generalized Kuramoto-Sivashinsky equation using B-spline functions*, Appl. Math. Model. 36 (2012), pp. 605–617.
[16] R.C. Mittal and G. Arora, *Quintic B-spline collocation method for numerical solution of the Kuramoto-Sivashinsky equation*, Commun. Nonlinear Sci. Numer. Simul. 15 (2010), pp. 2798–2808.
[17] R.C. Mittal and S. Dahiya, *A quintic B-Spline based differential quadrature method for numerical solution of Kuramoto-Sivashinsky equation*, Int. J. Nonlinear Sci. Numer. Simul. 18 (2017), pp. 103–114.
[18] R.K. Mohanty, W. Dai and F. Han, *A new high accuracy method for two-dimensional biharmonic equation with nonlinear third derivative terms: Application to Navier-Stokes equations of motion*, Int. J. Comput. Math. 92 (2015), pp. 1574–1590.
[19] R.K. Mohanty and D. Kaur, *High accuracy implicit variable mesh methods for numerical study of special types of fourth order non-linear parabolic equations*, Appl. Math. Comput. 273 (2016), pp. 678–696.
[20] R.K. Mohanty, D. Kaur, *A class of quasi-variable mesh methods based on off-step discretization for the numerical solution of fourth-order quasi-linear parabolic partial differential equations*. Adv. Differ. Equ. 2016 (2016), pp. 326, 29
[21] R.K. Mohanty and D. Kaur, *Numerov type variable mesh approximations for 1D unsteady quasi-linear biharmonic problem: application to Kuramoto-Sivashinsky equation*, Numer. Algor. 74 (2017), pp. 427–459.
[22] J. Rashidinia and M. Jokar, *Polynomial scaling functions for numerical solution of generalized Kuramoto-Sivashinsky equation*, Appl. Anal. 96 (2017), pp. 293–306.
[23] S. Saprykin, E.A. Demekhin and S. Kalliadasis, *Two-dimensional wave dynamics in thin films, I. Stationary solitary pulses*, Phys. Fluids 17 (2005), pp. 117105.
[24] G. Sivashinsky, *Nonlinear analysis of hydrodynamic instability in laminar flames, Part I, Derivation of basic equations*, Acta Astronaut. 4 (1977), pp. 1177–1206.
[25] T. Tatsumi, *Irregularity, regularity and singularity of turbulence, turbulence and chaotic phenomena in fluids*, Iutam. (1984), pp. 1–10.
[26] M. Uddin, S. Haq, Siraj-ul-Islam, *A mesh-free numerical method for solution of the family of Kuramoto-Sivashinsky equations*, Appl. Math. Comput. 212 (2009), pp. 458–469.
[27] Y. Xu and C.W. Shu, *Local discontinuous Galerkin methods for the Kuramoto-Sivashinsky equations and the Ito-type coupled KdV equations*, Comput. Methods Appl. Mech. Eng. 195 (2006), pp. 3430–3447.
[28] W. Zimmerman, *Propagating fronts near a Lifshitz point*, Phys. Rev. Lett. 66 (1991), pp. 1546.